

Research in Astronomy and Astrophysics manuscript no.
 (L^AT_EX: RAA20170134.tex; printed on December 5, 2017; 1:38)

Multi-color light curves and orbital period research of eclipsing binary V1073 Cyg

Xiao-man Tian^{1,2,3}, Li-ying Zhu^{1,2,3}, Sheng-bang Qian^{1,2,3}, Lin-jia Li^{1,2,3} and Lin-qiao Jiang⁴

¹ Yunnan Observatories, Chinese Academy of Sciences (CAS), P. O. Box 110, 650216 Kunming, China;
joie@ynao.ac.cn

² Key Laboratory of the Structure and Evolution of Celestial Objects, Chinese Academy of Sciences, P. O. Box 110, 650216 Kunming, China

³ University of the Chinese Academy of Science, Yuquan Road 19, Sijingshang Block, 100049 Beijing, China

⁴ School of Physics and Electronic Engineering, Sichuan University of Science & Engineering, Zigong 643000, China

Abstract New Multi-color B V R_c I_c photometric observation are presented for W UMa type eclipsing binary V1073 Cyg. The multi-color light curves analysis with the Wilson-Devinney(W-D) procedure acquired the absolute parameters of this system, showing that V1073Cyg is a shallow contact binary system with fill-out factor $f = 0.124(\pm 0.011)$. We collected all available times of light minima spanning 119 years including CCD data to construct the O-C curve and made detailed O-C analysis. The O-C diagram shows that the period change is complex. There exist a long-term continuous decrease and a cyclic variation. The period is decreasing at a rate of $\dot{P} = -1.04(\pm 0.18) \times 10^{-10} \text{days} \cdot \text{cycle}^{-1}$, and with the period decrease, V1073 Cyg will evolve to deep contact stage. The cyclic variation with a period of $P_3 = 82.7(\pm 3.6) \text{years}$ and an amplitude of $A = 0.028(\pm 0.002) \text{day}$ may be explained by the magnetic activity of one or both components or the light travel time effect (LTTE) caused by a distant third companion with $M_3(i' = 90^\circ) = 0.511M_\odot$.

Key words: star: binaries: close-star: binaries: eclipse-star: binaries: individual(V1073 Cyg)

1 INTRODUCTION

V1073 Cyg (BD +33° 4252, HD 204038, HIP 105739, BV 342) is a W UMa type eclipsing binary. Strohmeier (1960) first recognized the variability of V1073 Cyg, then the photographic light curve was published in 1962 (Strohmeier, 1962). Thus far, more photometric and spectrographic researches have been carried out for V1073 Cyg (such as Sezer (1993); Morris & Naftilan (2000); Yang & Liu (2000); Ekmekçi (2012) and so on), and absolute parameters have been derived. Here are the brief introduction. Radial veloc-

$q = 0.303(17)$ was presented by Pribulla et al. (2006) based on their radial-velocity curve. And the fill-out factor has been reported many times, such as $f = 0.007$ and $f = 0.008$ (Kondo, 1966; Leung & Schneider, 1978; Ahn et al., 1992; Sezer, 1993, 1994), $f = 0.19$ (Jafari et al., 2006), and $f = 0.20$ (Sezer, 1996). The original classification of the spectral type of the primary star was A3 Vm (Fitzgerald, 1964), some other spectral types classification also were reported as F0n III-IV (Abt et al., 1969), F0n V (Morgan et al., 1943) and F0V (Pribulla et al., 2006). Investigations about V1073 Cyg have confirmed that this system is a short-period contact eclipsing system with a period of $P = 0.7858506\text{day}$ (Pribulla et al., 2006).

The orbital period analysis has been taken out by many authors. Aslan & Herczeg (1984) found that the period decreased about 0.4 seconds in 1976 using 25 photoelectric and some photograph epochs of minima since 1962, then Wolf & Diethelm (1992) made a new O-C analysis with adding 16 photoelectric times of light minima and detected a constant decrease. One year later, Sezer (1993) made a analysis using 29 photoelectric data and reported that the period was decreasing by $3.12(\pm 0.17)$ seconds per century (i.e. $\dot{P} = -7.8 \times 10^{-10} \text{ days} \cdot \text{cycle}^{-1}$). 17 years ago, Morris & Naftilan (2000) pointed out that the period had decreased $0.795 \pm 0.040\text{s}$ around JD 2,445,000 in 1982, while Yang & Liu (2000) found that the period was decreasing at a rate of $\dot{P} = -8.8 \times 10^{-10} \text{ days} \cdot \text{cycle}^{-1}$ from 1962 to 1998 year, using 111 data including 62 pe data in their analysis. By now, more high-precision eclipse times have been obtained, which are very useful for more precise period investigation.

According to the spectroscopic observation made by Fitzgerald (1964), the spectrum of the primary component shows that the primary component of V1073 Cyg is a Am star. V1073 Cyg has been listed in the catalog of Ap, HgMn and Am stars (Renson & Manfroid, 2009) as a doubtful Am star. Am stars almost are A and F type stars with remarkable peculiar characteristic of element abundances, such as considerably weaker Ca II, K line (Titus & Morgan, 1940; Roman et al., 1948), under-abundance of calcium and scandium, over-abundances of iron-group elements, and extreme enhancements of rare-earth elements (Conti, 1970) compared to the same spectral type stars. Am stars rotate more slow than normal A and F type stars, and the rotational velocities are always less than about $100\text{km} \cdot \text{s}^{-1}$ (Abt & Moyd, 1973); Am stars show high binaries-proportion, which is more than 90% (Abt, 1961, 1965; Hubrig et al., 2010). As the only one W UMa type binary of the 73 eclipsing Am binaries (Renson & Manfroid, 2009; Smalley et al., 2014), V1073 Cyg is very special because the rotation velocity of the primary component is about $160\text{ km} \cdot \text{s}^{-1}$ (Pribulla et al., 2006), which is much higher than the limit rotation velocity $100\text{km} \cdot \text{s}^{-1}$ given by Abt & Moyd (1973), that makes it became a challenge to the cut-off of rotation velocity. So the investigations both photometric and spectroscopic of this target are very important.

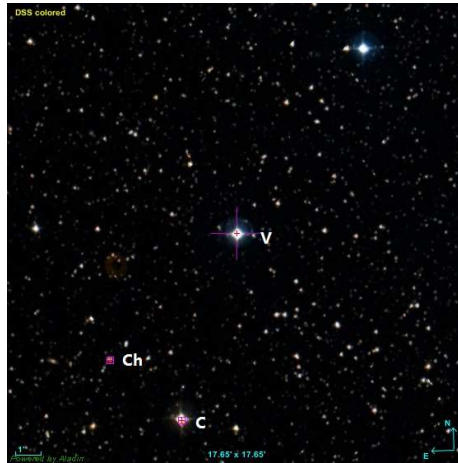
In this study, we carried out a new photometric solution for V1073 Cyg based on our new multi-color light curves and derived new absolute parameters. We also collected the times of minima of V1073 Cyg spanning 119 years and made a new exhaustive orbital period analysis.

2 OBSERVATION AND DATA REDUCTION

Four filters light curve observations of V1073 Cyg were carried out on 2015 October 26, 27, 28, 29 using the Andor DZ936 2K CCD (size: 2048×2048 pixel) photometric system attached to the 85 cm telescope

Table 1 The information of V1073 Cyg, comparison and check stars

	Variable(V)	Comparison(C)	Check(Ch)
	V1073 Cyg	BD+32 4152	TYC 2707-276-1
α_{2000}	$21^h 25^m 00^s.35766$	$21^h 25^m 10^s.6007$	$21^h 23^m 10^s.72$
δ_{2000}	$+33^\circ 41' 14'' .9435$	$+33^\circ 34' 09'' .306$	$+33^\circ 23' 29'' .9$
V(mag)	8. 38	8. 77	12.18

**Fig.1** Finding chart. 'V','C' and 'Ch' represent 'Variable star','Comparison star' and 'Check star' respectively.

And observations of minima light times were carried out on 2015 June 17 using '*D80cm*' and on 2015 September 28 using the Andor DW436 2K CCD camera mounted in the 60 cm reflecting telescope (labeled as '*D60cm*') at the Yunnan Observatories in China (YNO). The images were processed with the PHOT package of IRAF in a standard mode. Then, differential magnitudes were determined, by choosing BD+32 4152 as the comparison star and TYC 2707-276-1 as the check star. The relevant information are listed in Table 1 and the finding chart is shown in Figure 1.

3 LIGHT CURVES AND ANALYSES

New multi-color curves of V1073 Cyg were obtained in this study. The photometric phases were calculated with the new linear ephemeris:

$$\text{Min}I = 2457191.2159(.0003) + 0.^d7858506 * E \quad (1)$$

in which, 2457191.2159 is the new time of light minima obtained by this study, and $P = 0.7858506\text{day}$

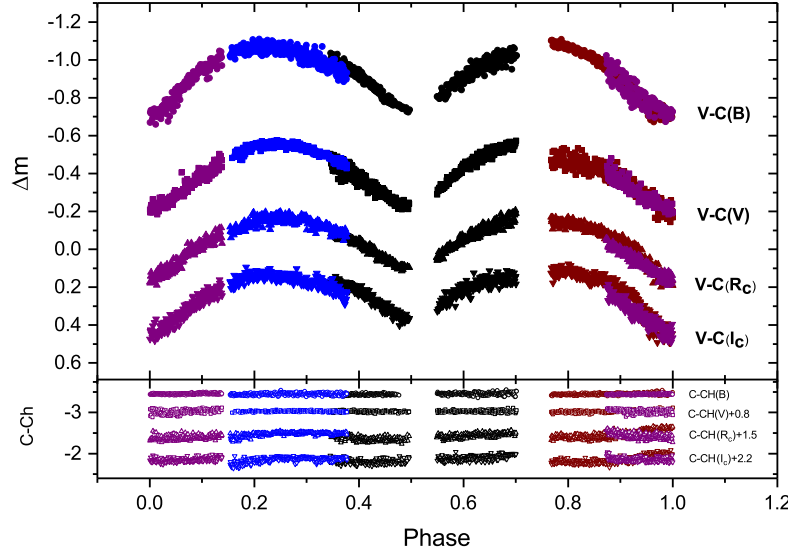


Fig. 2 The phased light curves of V1073 Cyg. Circle, square, triangle and down triangle represent B V R_c I_c bands observation data and the open symbols show the corresponding magnitude differences between comparison star and check star.

in Figure 2 with different color marking the observations of different day, and corresponding magnitude differences between comparison star and check star are shown in the bottom panel.

Absolute parameters of this system were derived from the light curves analysis with Mode 3 in the Wilson-Devinney(W-D) program (Wilson & Devinney, 1971; Wilson, 1979, 1990; Van Hamme & Wilson, 2007; Wilson, 2008; Wilson et al., 2010; Wilson, 2012). In the solution process, we adopted $q=0.303$ and F0 V as the spectral type of primary star (Pribulla et al., 2006). Then refer to the Table 15.7 (Calibration of MK spectral types) in the book named Allen's Astrophysical Quantities by Cox (1999), the temperature of primary star (star 1 in Mode 3) should be $T_1 = 7300K$, the convergent photometric solutions are derived and listed in Table 2. We tried to set the third light l_3 as a free parameter, but failed to obtain the convergent solution. Based on the Kepler's third law and $(M_1 + M_2)\sin i^3 = 1.896(25)$ (Pribulla et al., 2006), the absolute parameters (M_1 , M_2 , R_1 , R_2 , a) can be derived, which are listed in Table 2. The theoretical light curves are plotted in Figure 3, while the geometrical structure is shown in Figure 4.

4 O-C DIAGRAM ANALYSES

We collected 257 times of light minima from 1899 to 2017 and observed three times in 2015. All these 260 times of light minima were listed in Table 3. The time HJD 2447408.7690 observed by spectrographic method was abandoned because of the obvious deviation from the O-C diagram, and all the others listed in the Table 3 were used for the O-C analysis. The O-C values were determined by the observed (O) mid-eclipse times minus the calculated (C) times with Ephemeris(1). The corresponding O-C diagram is shown in the upper panel of Figure 5 with spot, triangle, pentagram and down triangle representing the CCD , pe ,

Table 2 Photometric Solutions of V1073 Cyg

Parameter	Value
Mode	3
$q(M_2/M_1)$	0.303(fixed)
$M_1(M_\odot)$	1.810 (± 0.004)
$M_2(M_\odot)$	0.549 (± 0.001)
$R_1(R_\odot)$	2.545(± 0.008)
$R_2(R_\odot)$	1.481(± 0.009)
$a(R_\odot)$	5.172(± 0.030)
$i(^{\circ})$	68.4(± 0.1)
$T_1(K)$	7300
$T_2(K)$	6609(± 18)
$\Omega_{\text{ega}1}$	2.450(± 0.002)
$L_1/L_{\text{total}}(B)$	0.832(± 0.002)
$L_1/L_{\text{total}}(V)$	0.829(± 0.002)
$L_1/L_{\text{total}}(R_c)$	0.804(± 0.002)
$L_1/L_{\text{total}}(I_c)$	0.794 (± 0.003)
$f(\text{fill-out})$	0.124 (± 0.011)
$r_1(\text{pole})$	0.460 (± 0.0005)
$r_1(\text{side})$	0.496 (± 0.0006)
$r_1(\text{back})$	0.522 (± 0.0008)
$r_2(\text{pole})$	0.267 (± 0.0005)
$r_2(\text{side})$	0.279 (± 0.0006)
$r_2(\text{back})$	0.315 (± 0.0010)
$\sum(O - C)^2$	0.035

The period decrease had been well discussed (Aslan & Herczeg, 1984; Wolf & Diethelm, 1992; Sezer, 1993; Morris & Naftilan, 2000; Yang & Liu, 2000). We tried to fit the O-C curve with downward parabola curve indicating period decrease, which is shown with dished line in the upper panel of Figure 5. The residuals $(O - C)_1$ from the parabolic fit are displayed in the middle panel, which also show a cyclic oscillation indicating the existence of a cyclic variation. So we combined the downward parabola curve with a cyclic variation and tried to make a good fit to the general trend of the O-C curve. The combination curve is plot in the upper panel of Figure 5 with solid line. Taking the case (eccentric orbital) reported by Qian (2015) into account, following equation (2) was used to describe the O-C diagram:

$$O - C = \Delta T_0 + \Delta P_0 \times E + 1/2\beta E^2 + \tau \quad (2)$$

ΔT_0 is the corresponding correction values of the epoch and ΔP_0 is the period in Equation(1), β is the

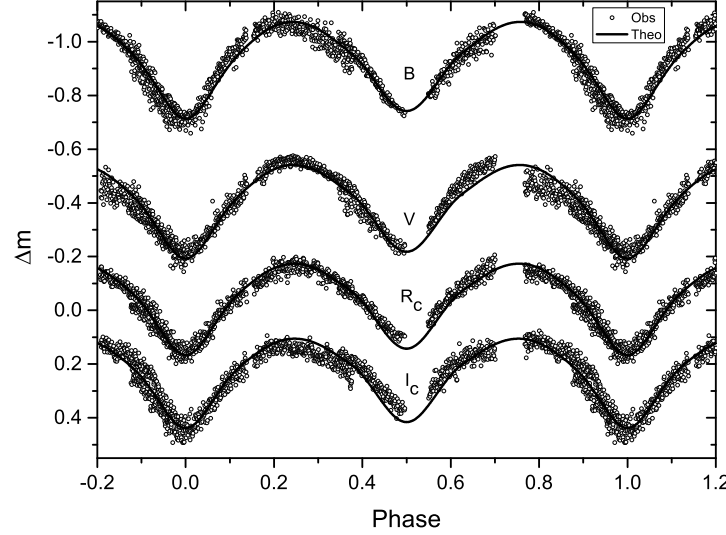


Fig.3 The observed (circles) and theoretical light curves (solid lines) of V1073 Cyg.

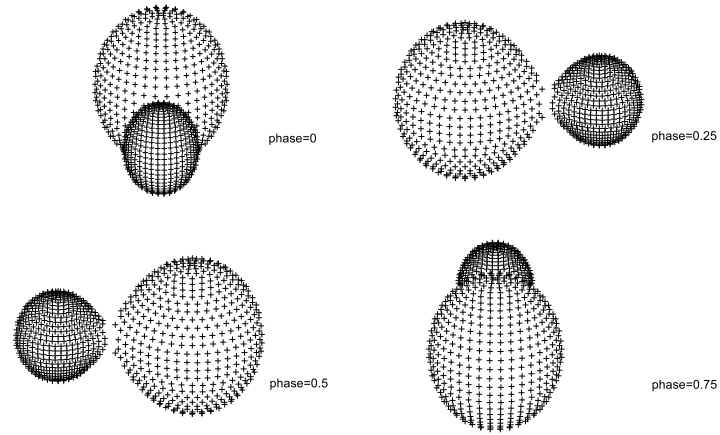


Fig.4 Geometrical structure of V1073 Cyg at phases 0.0, 0.25, 0.5 and 0.75 respectively.

time effect (LTTE) (Irwin, 1952a), shown as $(O - C)_1$ in the middle panel of Figure 5,

$$\tau = A[(1 - e^2) \frac{\sin(\nu + \omega)}{1 + e \cos(\nu)} + e \sin(\omega)] \quad (3)$$

$$= A[\sqrt{(1 - e^2)} \sin E^* \cos \omega + \cos E^* \sin \omega] \quad (4)$$

in which, $A = a_{12}' \sin i' / c$ (day) is the projected semi-major axis and c is the velocity of light, e , ν , ω

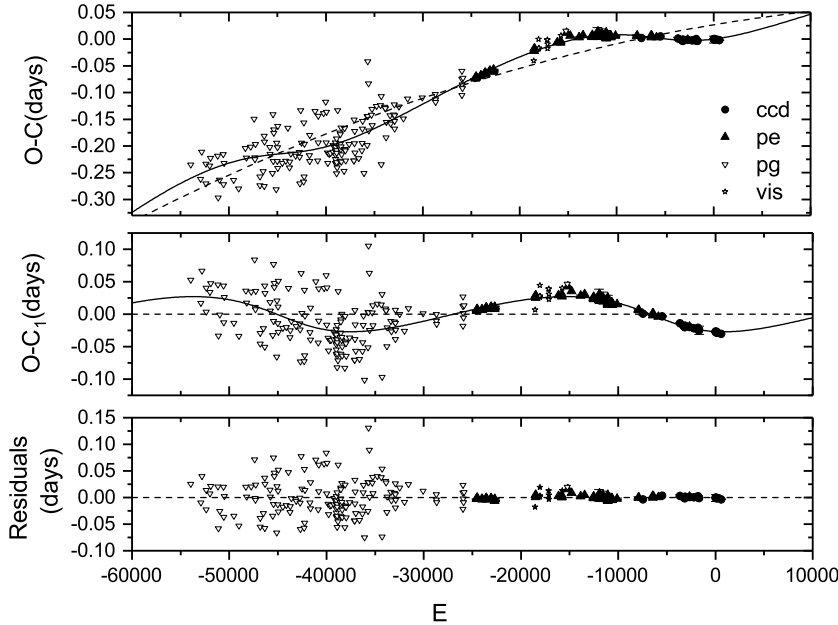


Fig. 5 O-C diagram of V1073 Cyg. Spots, triangle, open down triangle and pentagram mark the *CCD*, *pe*, *ph* and *vis* data respectively. The solid line showing in the upper panel is the combination of the continuous decrease and the cyclic variation, while the sine-like curve showing in the middle panel refers to the cyclic variation ($O - C$)₁ after the subtraction of the continuous decrease, and the residuals are shown in the bottom panel.

anomaly. The Kepler equation leads to the relationship formula of the mean anomaly M and E^* :

$$M = E^* - e \sin E^* = \frac{2\pi}{P_A}(t - T) \quad (5)$$

P_A is the anomalistic period, t is the time of light minimum, and T is the time of periastron passage respectively.

In our O-C analysis, we adopt different weight for different-precision data, i.e. a weight of 5 for CCD (ccd) and photoelectric (pe) data and a low weight of 1 for visual (vis) and photographic (pg) data, as same as that of Yang & Liu (2000). The combination of the change of continuum decrease and cyclic variation gives a good fit to the O-C curve. All the fitting curves have been shown in Figure 5, the solid line showing in the upper panel refers to the combination of the continuous decrease with a rate of $\dot{P} = -1.04(\pm 0.18) \times 10^{-10} \text{ days} \cdot \text{cycle}^{-1}$ and the cyclic variation with a period of $P_3 = 82.7(\pm 3.6) \text{ years}$ and an amplitude of $A = 0.028(\pm 0.002) \text{ day}$. While the curve showing in the middle panel is the cyclic variation ($O - C$)₁ after subtracting the continuous decrease, and the residuals are shown in the bottom panel. And all results obtained from the above period analysis are listed in Table 4.

5 DISCUSSION AND CONCLUSION

V1073 Cyg is a short-period W UMa type eclipsing binary with a period of $P = 0.7858506 \text{ day}$. Our new multi-color light curves analysis found that V1073 Cyg is a shallow contact binary, with a fill-out factor of $f(\text{fill-out}) = 0.124(\pm 0.011)$, an orbit inclination angle of $i = 68.4(\pm 2.9)^\circ$ and $M_1 = 1.810(\pm 0.004) M_\odot$,

Table 3 The times of light minima of V1073 Cyg

HJD (2,400,000+)						HJD (2,400,000+)					
Error	Min.	Meth.	E	O-C(day)	Ref.	Error	Min.	Meth.	E	O-C(day)	Ref.
14801.8070	s	pg	-53940.5	-0.23464	1	23641.8050	s	pg	-42691.5	-0.27004	1
15601.7760	s	pg	-52922.5	-0.26155	1	23725.6350	p	pg	-42585	-0.13313	1
15694.5570	s	pg	-52804.5	-0.21092	1	23773.5110	p	pg	-42524	-0.19402	1
16029.6630	p	pg	-52378	-0.27021	1	23953.7910	s	pg	-42294.5	-0.26673	1
16033.6290	p	pg	-52373	-0.23346	1	23981.7990	p	pg	-42259	-0.15643	1
16330.6770	p	pg	-51995	-0.23698	1	24003.7020	p	pg	-42231	-0.25724	1
16413.5990	s	pg	-51889.5	-0.22222	1	24016.7300	s	pg	-42214.5	-0.19578	1
16990.8100	p	pg	-51155	-0.21849	1	24422.6000	p	pg	-41698	-0.21761	1
17021.7730	s	pg	-51115.5	-0.29659	1	24459.5240	p	pg	-41651	-0.22859	1
17145.5780	p	pg	-50958	-0.26306	1	24459.5730	p	pg	-41651	-0.17959	1
17432.8540	s	pg	-50592.5	-0.21545	1	24889.4780	p	pg	-41104	-0.13487	1
17458.7310	s	pg	-50559.5	-0.27152	1	25102.7440	s	pg	-40832.5	-0.22731	1
17497.6700	p	pg	-50510	-0.23213	1	25132.6900	s	pg	-40794.5	-0.14363	1
18283.4890	p	pg	-49510	-0.26373	1	25139.7130	s	pg	-40785.5	-0.19329	1
18683.4710	p	pg	-49001	-0.27968	1	25573.5570	s	pg	-40233.5	-0.13882	1
19238.7500	s	pg	-48294.5	-0.20413	1	25748.8230	s	pg	-40010.5	-0.11750	1
19308.6730	s	pg	-48205.5	-0.22183	1	25779.7880	p	pg	-39971	-0.19360	1
19668.6130	s	pg	-47747.5	-0.20141	1	25803.8140	s	pg	-39940.5	-0.13604	1
19948.8210	p	pg	-47391	-0.14915	1	25890.5740	p	pg	-39830	-0.21253	1
20005.7230	s	pg	-47318.5	-0.22132	1	25925.5250	s	pg	-39785.5	-0.23189	1
20012.7920	s	pg	-47309.5	-0.22497	1	26029.6670	p	pg	-39653	-0.21509	2
20046.6120	s	pg	-47266.5	-0.19655	1	26127.5070	s	pg	-39528.5	-0.21349	2
20407.6330:	p	pg	-46807	-0.27390	1	26352.2630	s	pg	-39242.5	-0.21076	2
20409.6140:	s	pg	-46804.5	-0.25752	1	26352.2750	s	pg	-39242.5	-0.19876	2
20667.7760	p	pg	-46476	-0.24745	1	26444.6100	p	pg	-39125	-0.20121	2
20763.6220:	p	pg	-46354	-0.27522	1	26547.5260	p	pg	-38994	-0.23164	2
20769.6100	s	pg	-46346.5	-0.18110	1	26547.5330	p	pg	-38994	-0.22464	2
20789.6380	p	pg	-46321	-0.19229	1	26547.5410	p	pg	-38994	-0.21664	2
21206.5220	s	pg	-45790.5	-0.20203	1	26547.5490	p	pg	-38994	-0.20864	2
21228.5130	s	pg	-45762.5	-0.21485	1	26547.5560	p	pg	-38994	-0.20164	2
21423.7610	p	pg	-45514	-0.25072	1	26547.5640	p	pg	-38994	-0.19364	2
21481.6310:	s	pg	-45440.5	-0.14074	1	26619.4290	s	pg	-38902.5	-0.23397	2
21488.6160	s	pg	-45431.5	-0.22840	1	26623.3410	s	pg	-38897.5	-0.25122	2
21542.5060	p	pg	-45363	-0.16916	1	26623.3620	s	pg	-38897.5	-0.23022	2
21544.4640	s	pg	-45360.5	-0.17579	1	26623.3840	s	pg	-38897.5	-0.20822	2
21731.7840:	p	pg	-45122	-0.28116	1	26623.4060	s	pg	-38897.5	-0.18622	2
21768.8060	p	pg	-45075	-0.19414	1	26624.5580	p	pg	-38896	-0.21299	2
21825.7460	s	pg	-45002.5	-0.22831	1	26675.2180	s	pg	-38831.5	-0.24036	2
21844.6320	s	pg	-44978.5	-0.20272	1	26711.4740	s	pg	-38785.5	-0.13349	1
21859.6030	s	pg	-44959.5	-0.16288	1	26861.5020	s	pg	-38594.5	-0.20295	2
21866.5970	s	pg	-44950.5	-0.24154	1	26913.7890	p	pg	-38528	-0.17502	1
22238.7070	p	pg	-44477	-0.23180	1	26915.3080	p	pg	-38526	-0.22772	2
22511.7940	s	pg	-44129.5	-0.22788	1	26926.7350	s	pg	-38511.5	-0.19555	1
22674.5270	s	pg	-43922.5	-0.16595	1	26929.5030	p	pg	-38508	-0.17803	2
22819.8350	s	pg	-43737.5	-0.24031	1	26979.3760	s	pg	-38444.5	-0.20654	2
22834.7770	s	pg	-43718.5	-0.22948	1	27000.2420	p	pg	-38418	-0.16558	2
22924.7720	p	pg	-43604	-0.21437	1	27002.5640	p	pg	-38415	-0.20113	1
23308.6560	s	pg	-43115.5	-0.21839	1	27026.5040	s	pg	-38384.5	-0.22958	1
23612.7870	s	pg	-42728.5	-0.21157	1	27036.3410	p	pg	-38372	-0.21571	1
23638.7110	s	pg	-42695.5	-0.22064	1	27241.8100:	s	pg	-38110.5	-0.24664	1

Table 3 Continued

HJD (2, 400, 000+)						HJD (2, 400, 000+)						
Error	Min.	Meth.	E	O-C(day)	Ref.	Error	Min.	Meth.	E	O-C(day)	Ref.	
27267.8230	s	pg	-38077.5	-0.16671	1	34653.2960	s	pg	-28679.5	-0.11765	2	
27272.4990	s	pg	-38071.5	-0.20581	1	36788.4650	s	pg	-25962.5	-0.10473	2	
27313.3620	s	pg	-38019.5	-0.20705	1	36788.5100	s	pg	-25962.5	-0.05973	2	
27333.4000	p	pg	-37994	-0.20824	1	36790.4600	p	pg	-25960	-0.07436	2	
27354.5990	p	pg	-37967	-0.22720	1	36814.4180	s	pg	-25929.5	-0.08480	2	
27632.8210	p	pg	-37613	-0.19631	1	36840.3440	s	pg	-25896.5	-0.09187	2	
28027.6800	s	pg	-37110.5	-0.22724	1	36868.2610	p	pg	-25861	-0.07257	2	
28032.7880	p	pg	-37104	-0.22727	1	37878.4707	0.0004	s	pe	-24575.5	-0.07381	3
28062.7270	p	pg	-37066	-0.15059	1	37928.3750	p	pe	-24512	-0.07102	4	
28064.6470	s	pg	-37063.5	-0.19522	1	37935.4480	p	pe	-24503	-0.07068	4	
28090.6030	s	pg	-37030.5	-0.17229	1	37939.3762	0.0005	p	pe	-24498	-0.07173	3
28126.3190	p	pg	-36985	-0.21249	1	37941.3401	0.0011	s	pe	-24495.5	-0.07246	3
28429.6470	p	pg	-36599	-0.22282	1	38327.5890	p	pe	-24004	-0.06823	2	
28668.5600	p	pg	-36295	-0.20841	1	38353.5219	p	pe	-23971	-0.06930	4	
28694.5070	p	pg	-36262	-0.19447	1	38662.3674	p	pe	-23578	-0.06309	4	
28729.5040	s	pg	-36217.5	-0.16783	1	38669.4397	p	pe	-23569	-0.06344	4	
28753.4870	p	pg	-36187	-0.15327	1	38672.5820	p	pe	-23565	-0.06454	2	
28844.5480	p	pg	-36071	-0.25094	1	38692.6208	s	pe	-23539.5	-0.06493	2	
29111.4510	s	pg	-35731.5	-0.14422	1	38707.5520	s	pe	-23520.5	-0.06489	2	
29114.5400	s	pg	-35727.5	-0.19862	2	38731.5204	p	pe	-23490	-0.06494	2	
29159.3880	s	pg	-35670.5	-0.14410	2	39040.3651	p	pe	-23097	-0.05952	4	
29161.4550	p	pg	-35668	-0.04173	2	39077.3002	p	pe	-23050	-0.05940	4	
29212.4940:	p	pg	-35603	-0.08302	1	39338.5946	0.0009	s	pe	-22717.5	-0.06033	3
29244.2330	s	pg	-35562.5	-0.17097	2	39340.5613	0.0014	p	pe	-22715	-0.05825	3
29465.4790	p	pg	-35281	-0.14191	2	39342.5232	0.0010	s	pe	-22712.5	-0.06098	3
29491.4230	p	pg	-35248	-0.13098	2	39355.4932	0.0016	p	pe	-22696	-0.05751	3
29516.5400	p	pg	-35216	-0.16120	2	42616.3970:	s	vis	-18546.5	-0.04078	5	
29857.6350	p	pg	-34782	-0.12536	1	42660.4276	s	pe	-18490.5	-0.01781	6	
30181.8000	s	pg	-34369.5	-0.12374	1	42662.3880	p	pe	-18488	-0.02204	6	
30251.6300	s	pg	-34280.5	-0.23444	1	42671.4289	s	pe	-18476.5	-0.01842	6	
30259.6160	s	pg	-34270.5	-0.10694	1	43005.4150	s	vis	-18051.5	-0.01883	7	
30533.4650	p	pg	-33922	-0.12688	1	43012.5060	s	vis	-18042.5	-0.00048	7	
30576.6840	p	pg	-33867	-0.12966	1	43014.4540	p	vis	-18040	-0.01711	7	
30583.7570	p	pg	-33858	-0.12932	1	43016.4190	s	vis	-18037.5	-0.01673	7	
30648.5350	s	pg	-33775.5	-0.18399	1	43715.4480	p	vis	-17148	-0.00184	8	
30663.4950	s	pg	-33756.5	-0.15515	1	43722.5210	p	vis	-17139	-0.00150	9	
30965.6670	p	pg	-33372	-0.14271	1	43731.5420	s	vis	-17127.5	-0.01778	9	
30983.7290	p	pg	-33349	-0.15527	1	43744.5170	p	vis	-17111	-0.00932	8	
31004.5510	s	pg	-33322.5	-0.15831	1	44506.7950	p	pe	-16141	-0.00640	10	
31247.7890	p	pg	-33013	-0.14107	1	44783.4139	p	pe	-15789	-0.00691	10	
31319.7130	s	pg	-32921.5	-0.12240	1	44790.4489	p	pe	-15780	-0.00356	10	
31323.5970	s	pg	-32916.5	-0.16766	1	44816.4330	p	vis	-15747	0.00647	11	
31328.7300	p	pg	-32910	-0.14269	1	45216.4400	p	pg	-15238	0.01551	12	
31341.6860	s	pg	-32893.5	-0.15322	1	45275.3750	p	pe	-15163	0.01172	13	
31673.7350	p	pg	-32471	-0.12610	1	45568.8845	s	pe	-14789.5	0.00602	14	
32053.6710	s	pg	-31987.5	-0.14886	1	46291.4714	0.0010	p	pe	-13870	0.00329	15
32381.8010	p	pg	-31570	-0.11149	1	46614.4600	p	pe	-13459	0.00729	16	
33575.5100	p	pg	-30051	-0.10955	1	47326.4385	p	pe	-12553	0.00515	17	
34636.4150	p	pg	-28701	-0.10286	2	47348.4413	p	pe	-12525	0.00413	17	
34651.3360	p	pg	-28682	-0.11302	2	47350.4067	s	pe	-12522.5	0.00491	17	

Table 3 Continued

HJD (2, 400, 000+)						HJD (2, 400, 000+)							
Error	Min.	Meth.	E	O-C(day)	Ref.	Error	Min.	Meth.	E	O-C(day)	Ref.		
47357.4820	s	pe	-12513.5	0.00755	17	48864.3487	0.0008	p	pe	-10596	0.00573	20	
47377.5175	p	pe	-12488	0.00386	17	48865.5247	0.0013	s	pe	-10594.5	0.00295	20	
47408.7690	p	sp	-12448	-0.17866	18	49236.4492	0.0014	s	pe	-10122.5	0.00597	20	
47748.4413	p	pe	-12016	0.00618	19	50968.8568	0.0020	p	pe	-7918	0.00592	26	
47761.4060	0.0010	s	pe	-11999.5	0.00434	20	51001.8627	0.0005	p	pe	-7876	0.00609	26
47763.3764	0.0008	p	pe	-11997	0.01012	20	51326.4150		p	ccd	-7463	0.00210	27
47776.3453	0.0009	s	pe	-11980.5	0.01248	20	52130.3446		p	pe	-6440	0.00653	28
47822.3117	p	pe	-11922	0.00662	21	52144.4867		p	pe	-6422	0.00332	28	
47822.3191	p	pe	-11922	0.01402	21	52172.3871		s	pe	-6386.5	0.00602	28	
47840.3834	p	pe	-11899	0.00376	21	52569.6317		p	pe	-5881	0.00315	29	
47840.3840	p	pe	-11899	0.00436	21	52874.1509		s	ccd	-5493.5	0.00524	30	
48106.3953	0.0015	s	pe	-11560.5	0.00523	20	54317.3616	0.0020	p	ccd	-3657	0.00131	31
48106.4010	0.0080	s	pe	-11560.5	0.01093	3	54617.5533	0.0009	p	ccd	-3275	-0.00192	32
48115.4316	p	pe	-11549	0.00425	19	54697.3165	0.0002	s	ccd	-3173.5	-0.00255	33	
48132.3293	0.0027	s	pe	-11527.5	0.00616	20	54698.4943	0.0002	p	ccd	-3172	-0.00353	33
48145.2951	0.0010	p	pe	-11511	0.00542	20	54720.5010	0.0004	p	ccd	-3144	-0.00065	33
48482.4214	p	pe	-11082	0.00182	3	55083.5635	0.0005	p	pe	-2682	-0.00112	34	
48482.4268	0.0028	p	pe	-11082	0.00722	19	55089.4572	0.0008	s	ccd	-2674.5	-0.00130	35
48482.4272	p	pe	-11082	0.00762	20	55447.4114	0.0010	p	ccd	-2219	-0.00205	36	
48484.3885	0.0054	s	pe	-11079.5	0.00429	3	55774.3275	0.0007	p	ccd	-1803	0.00020	37
48484.3966	0.0036	s	pe	-11079.5	0.01239	20	55777.4684	0.0008	p	ccd	-1799	-0.00230	37
48488.3169	0.0014	s	pe	-11074.5	0.00344	20	55779.4327	0.0002	s	ccd	-1796.5	-0.00263	37
48489.4935	0.0018	p	pe	-11073	0.00126	20	55793.5788	0.0003	s	ccd	-1778.5	-0.00184	37
48500.5030	p	pe	-11059	0.00885	22	55799.4728		p	ccd	-1771	-0.00172	22	
48504.4299	0.0005	p	pe	-11054	0.00650	3	55873.3412		p	ccd	-1677	-0.00328	22
48532.3265	0.0007	s	pe	-11018.5	0.00540	3	57191.2159	0.0003	p	ccd	0	0.00000	38
48559.4382	p	pe	-10984	0.00526	23	57214.3977	0.0064	s	ccd	29.5	-0.00082	39	
48559.4387	p	pe	-10984	0.00576	23	57294.1623	0.0005	p	ccd	131	0.00002	38	
48598.3360	s	pe	-10934.5	0.00345	24	57324.0210	0.0006	p	ccd	169	-0.00123	38	
48823.4853	p	pe	-10648	0.00656	25	57644.64990	0.0002	p	ccd	577	-0.00183	40	

Notes: (1)Strohmeier & Bauernfeind (1968). (2) Kondo (1966). (3) Wolf & Diethelm (1992). (4) Kruseman (1968). (5) Bonneville et al. (1975). (6) Dumitrescu & Dinescu (1976). (7) Braune & Mundry (1979). (8) Braune & Mundry (1981). (9) GEOS EB 13. (10) Aslan & Herczeg (1984). (11) BAV-M 34. (12)BAV-M 36. (13)Diethelm et al. (1983). (14) Scarfe et al. (1984) (15) Pohl et al. (1987). (16)BBSAG 80. (17) Keskin & Pohl (1989). (18)Ahn et al. (1992). (19) Wunder et al. (1992). (20) Muyesseroglu et al. (1996). (21)BAV-M 56 (22)B.R.N.O. data. (23)BAV-M 60. (24) BBSAG 99. (25)Blattler (1992b) . (26) Nelson (1998). (27)Rotse. (28) Derman & Kalci (2003). (29)Nelson (2003) (30)VSOLJ 42. (31) Brát et al. (2007). (32)Brát et al. (2008). (33)Yilmaz et al. (2009). (34) Hubscher et al. (2010). (35)Gokay et al. (2010). (36)Gokay et al. (2012). (37) Liakos & Niarchos (2011). (38) This study. (39) Hubscher (2016). (40)Juryšek et al. (2017).

The O-C analysis demonstrated that the orbital period of V1073 Cyg is undergoing a continuous decrease and a cyclic variation simultaneously. The period decrease rate $\dot{P} = -1.04(\pm 0.18) \times 10^{-10} \text{ days} \cdot \text{cycle}^{-1}$ is approximately consistent with $\dot{P} = -7.8 \times 10^{-10} \text{ days} \cdot \text{cycle}^{-1}$ of Sezer (1993) and $\dot{P} = -8.8 \times 10^{-10} \text{ days} \cdot \text{cycle}^{-1}$ of Yang & Liu (2000). More high-precision data (20 CCD data and more pe data) with a longest time span (119 years) were used in our analysis, the results derived from our O-C analysis will be more reliable. The long-term period changes could be explained by the combined effects of angular momentum loss (AML) and mass transfer between two components. With period decrease, V1073

Table 4 Orbital parameters of V1073 Cyg for two O-C diagram analysis

Parameter	Value
Revised epoch, ΔT_0 (day)	0.026834(± 0.004848)
Revised period, ΔP_0 (days)	$3.0261848 (\pm 0.4545760) \times 10^{-6}$
Rate of the linear decrease, β (days \cdot cycle $^{-1}$)	$-1.04 (\pm 0.18) \times 10^{-10}$
Eccentricity, e_3	0.26(± 0.15)
Longitude of the periastron passage, ω_3 ($^{\circ}$)	197.9 (± 25.3)
Time of periastron passage, T_3	2453082.8 (± 2111.1)
Semi-amplitude, A (day)	0.028(± 0.002)
Orbital period, P_3 (years)	82.7(± 3.6)
Orbital semi-major axis, $a_{12}^{'} \sin i^{'}(\text{AU})$	4.84(± 0.34)
Mass function, $f(m)(M_{\odot})$	0.017(± 0.004)
Mass, $M_3(i^{'} = 90^{\circ})(M_{\odot})$	0.511
orbital radius, $a_3(i^{'} = 90^{\circ})(\text{AU})$	22.368

single star, like V1309 Sco (Zhu et al., 2016). Long-term period variation (no matter decrease or increase) are very common for W UMa-type contact binaries, like V502 Oph(Derman & Demircan, 1992), V417 Aql (Qian, 2003), V1191 Cyg(Zhu et al., 2011), EP And (Liao et al., 2013), TY UMa(Samec et al., 2000), DD Ind (Samec et al., 2016) and so on.

The cyclic variation curve fits the O-C diagram very well in Figure 5, and this is the first time to detect a cyclic variation for V1073 Cyg. The period of the cyclic variation is $P_3 = 82.7(\pm 3.6)$ years and the corresponding amplitude $A = 0.028(\pm 0.002)$ day. There are two possible ways to interpret the cyclic variation, i.e. the magnetic activity of one or both components (Applegate , 1992), and the LTTE through the presence of a tertiary companion. In consideration of the short period and fast rotational velocity of about $160 \text{ km} \cdot \text{s}^{-1}$, and the constitution of a F0V type primary component and a late type secondary component, it is probable that magnetic activity cycles (Applegate , 1992; Lanza et al., 1998; Lanza & Rodonò, 1999) in the two components may appear in V1073 Cyg. Using the equation given by (Rovithis-Livaniou et al., 2000):

$$\Delta P = \sqrt{2[1 - \cos(2\pi P/P_3)]} \times A \quad (6)$$

In the formula, P_3 is the period of the cyclic oscillation, we can obtain the value of $\frac{\Delta P}{P}$. The variation of the quadruple momentum ΔQ causing such cyclic variation can be calculated with following equation (Lanza & Rodonò, 2002):

$$\frac{\Delta P}{P} = -9 \frac{\Delta Q}{Ma^2} \quad (7)$$

in which a is the separation between the two components. As $M_1 = 1.810 M_{\odot}$, $M_2 = 0.549 M_{\odot}$ and $a = 5.172 R_{\odot}$, combining the above two equations, $\Delta Q_1 = 3.6 \times 10^{52} \text{ gcm}^2$ and $\Delta Q_2 = 1.7 \times 10^{52} \text{ gcm}^2$ can be obtained for the components, and the values of ΔQ_1 and ΔQ_2 are typical ones for close binaries, for which the ΔQ should be about $10^{51} \sim 10^{52} \text{ gcm}^2$ (Lanza & Rodonò, 1999), so the Applegate mechanism

According to Liao & Qian (2010), the LTTE due to the existence of a distant third companion may be the plausible reason of the periodic variation of binaries. Third body plays an important role in the evolution of contact binaries. It will cause the periodic variation of period, and also will take away the angular momentum of system leading to the orbital contraction process and then promote the evolution of contact binaries (Tokovinin et al., 2006; Qian et al., 2013, 2014, 2017). In Table 2, $M_1 = 1.810(\pm 0.122)M_{\odot}$, and $M_2 = 0.549(\pm 0.037)M_{\odot}$, then the mass function of the tertiary companion can be calculated with the equation:

$$f(m) = \frac{4\pi^2}{GP_3^2} \times (a_{12}' \sin i')^3 = \frac{(M_3 \sin i')^3}{(M_1 + M_2 + M_3)^2} \quad (8)$$

In the formula, G is the gravitational constant, and P_3 is the orbital period of tertiary component. $a_{12}' \sin i' = 4.84(\pm 0.34)(AU)$ leads to $f(m) = 0.017(\pm 0.004)M_{\odot}$, and if $i' = 90^\circ$, then $M_3 = 0.511M_{\odot}$ and $a_3 = 21.368AU$ can be calculated out. This is the first time to detect the sign of the existence of a third body for V1073 Cyg. Our O-C analysis show that the mass of the third body is just little less than the mass of the second component, but we failed to fit the light curve with third light. No third body has been detected from the light curve analysis in the previous researches, and the radial velocity curves (Fitzgerald, 1964; Pribulla et al., 2006) didn't show any evidence of potential third body. One possible explanation is that the third body may exist as a white dwarf. In fact, the mass of the third body is around the mass peak distribution of dwarfs.

In our opinion, the LTTE will be more plausible than the magnetic activity mechanism to interpret the cyclic variation. Because, comparing with the magnetic cycles shown in solar-type single stars and close binaries (Maceroni et al., 1990; Bianchini, 1990), the period 82.7*years* of cyclic variation of V1073 Cyg is much long. LTTE may cause a strict cyclic variation of period not a simple period oscillation, which can be verify by more new CCD times of light minima data.

As we have mentioned that V1073Cyg is a special doubtful Am binary because of the fast rotation velocity. From our light curve and O-C curve analysis, we know that V1073Cyg is a shallow contact binary and the period is undergoing a long-term decrease. The mass transfer and loss occurring in this shallow contact binary will lead to the orbit shrinking. Because of the synchronous rotation, the components of V1073 Cyg will rotate faster, which makes V1073 Cyg more interesting.

Acknowledgements This work is partly supported by the Key Science Foundation of Yunnan Province (No. 2017FA001), Chinese Natural Science Foundation (Nos.11573063, 11325315 and U1631108) , CAS "Light of West China" Program, the research fund of Sichuan University of Science and Engineering (grant number 2015RC42).

New CCD photometric observations of the system were obtained with the 85 *cm* telescope at Xinglong station of National Astronomical Observatory and the 60 *cm* telescope in Yunnan Observatories.

References

- Abt, H. A., 1961, ApJS, 6, 37
- Abt, H. A., 1965, ApJS, 11, 429
- Abt, H. A., Bidelman, W.P., 1969, ApJ, 158, 1091
- Abt, H. A., Moyd, K. I. 1973, ApJ, 182, 809
- Ahn, Y. S.; Hill, G.; Khalesseh, B., 1992, A&A, 265, 597A
- Applegate J. H., 1992, ApJ, 385, 621
- Aslan, Z., Herczeg, T., 1984, IBVS, 2478, 1A
- Boeche, C., Grebel, E. K., 2016, A&A, 587A, 2B
- Blattler, E. 1992b, BBSAG, 101, 3
- Bianchini A., 1990, AJ, 99, 1941
- Bonneville, T., Chetanneau, A., Despres, F. et al. 1975, BBSAG, 23, 1B
- Brát, L., Zejda, M., Svoboda, P. 2007, OEJV, 74, 1
- Brát, L., Šmelcer, L., Kuèáková, H. et al. 2008, OEJV, 94, 1B
- Braune, W., J., Mundry, E. 1979, AN, 300, 165
- Braune, W., J., Mundry, E. 1981, AN, 302, 53
- Conti, P. S. 1970, PASP, 82, 781
- Cox, Arthur N., 1999, Allen's Astrophysical Quantities, Springer-Verlag
- Derman, E., Demircan, O., 1992, AJ, 103, 1658D
- Derman, E., Kalci, R. 2003, IBVS, 5439, 1
- Diethelm, R., Elias, D. P., Germann, R., et al. 1983, BBSAG, 64, 1
- Dumitrescu, A., Dinescu, R. 1976, IBVS, 1116, 1
- Ekmekçi, F., Elmasli, A., Yilmaz, M., 2012, NewA, 17, 603E
- Fitzgerald, M.P., 1964, PDDO.2, 417
- Gokay, G., Demircan, Y., Gursoytrak, H., et al. 2012, IBVS, 6039, 1
- Hubrig S., González J. F., Schóller M., et al. 2010, ASPC, 435, 257
- Hubscher, J., Lehmann, P. B., Monninger, G., et al. 2010, IBVS, 5941, 1
- Hubscher, Joachim, 2016, IBVS, 6157, 1H
- Irwin, J. B. 1952a, ApJ, 116, 211
- Jafari, M., Khalesseh, B., Pazhouhesh, R., 2006, Ap&SS, 306, 29J
- Juryšek, J., Hoñková, K., Šmelcer, L., et al., 2017, OEJV, 179, 1J
- Keskin, V., Pohl, E. 1989, IBVS, 3355, 1
- Kondo, Y., 1966, AJ, 71, 54
- Kruseman, P. 1968, BANS, 2, 377
- Gokay, G., Demircan, Y., Terzioglu, Z. et al. 2010, IBVS, 5922, 1G
- Lanza, A. F., Rodonò, M., & Rosnor, R. 1998, MNRAS, 296, 893
- Lanza A. F., Rodonò M., 1999, A&A, 349, 887
- Lanza A. F., Rodonò M., 2002, Astron. Nachr., 323, 424
- Leung, K.C., Schneider, D.P. 1978, ApJ, 222, 917

- Liao, W.P., Qian, S.-B. 2010, MNRAS, 405, 1930
- Liao, W-P., Qian, S.B., Li, K., et al. 2013, AJ, 146, 79L
- Liakos, A., Niarchos, P. 2011, IBVS, 6005, 1
- Maceroni C., Bianchini A., Rodono M., et al. 1990, A&A, 237, 395
- Morgan, W. W.; Keenan, P. C.; Kellman, E. 1943, An atlas of stellar spectra(Chicago: University of Chicago press)
- Morris, S. L., Naftilan, S. A. 2000, PASP, 112, 852
- Muyesseroglu, Z., Gurol, B., Selam, S. O. 1996, IBVS, 4380, 1
- Nelson, R. H. 1998, IBVS, 4621, 1
- Nelson, R. H. 2003, IBVS, 5371, 1
- Pohl, E., Akan, M. C., Ibanoglu, C., et al. 1987, IBVS, 3078, 1
- Pribulla, T., Rucinski, S. M., Lu, W., et al. 2006, AJ, 132, 769
- Qian, S. B. 2001b, MNRAS, 328, 635
- Qian, S. B. 2003, A&A, 400, 649
- Qian, S. B., Liu, N. P., Li, K., et al. 2013, ApJS, 209, 13Q
- Qian, S. B., Zhou, X., Zola, S., et al. 2014, AJ, 148, 79Q
- Qian, S. B., Han, Z. T., Fernández Lajús, E. et al. 2015, ApJS, 221, 17Q
- Qian, S. B., He, J. J., Zhang, J., et al. 2017, RAA, 17, 87
- Renson, P., Manfroid, J. 2009, A & A, 498, 961
- Roman, N. G., Morgan, W. W., & Eggen, O. J. 1948, ApJ, 107, 107
- Rovithis-Livaniou H., Kranidiotis A. N., Rovithis P., et al. 2000, A&A, 354, 904
- Samec, R. G., Stoddard, M. L., Faulkner, D. R. 2000, AAS Meeting Abstracts, 196, 4601S
- Samec, R. G., Norris, C. L., Van Hamme, W., et al. 2016, AJ, 152, 219S
- Scarfe, C. D., Forbes, D. W., Delaney, P. A., Gagne, J. 1984, IBVS, 2545, 1
- Sezer, C. 1993, Ap&SS, 208, 15
- Sezer, C. 1994, Ap&SS, 215, 153
- Sezer, C. 1996, Ap&SS, 245, 89
- Smalley, B., Southworth, J., Pintado, O. I. et al., 2014, A&A, 564A, 69S
- Strohmeier, W. 1960, Veroeffentlichungen der Remeis-Sternwarte zu Bamberg, Nr. 27. Veränderlichen-Colloquium Bamberg 1959. Bamberg, 1960, p.1
- Strohmeier, W. 1962, IBVS, 9
- Strohmeier, W., Bauernfeind, H. 1968, BamVe, 7, 72
- Titus, J., & Morgan, W. W. 1940, ApJ, 92, 256
- Tokovinin, A.; Thomas, S.; Sterzik, M.; Udry, S. 2006, A&A, 450, 681T
- Van H. W., Wilson, R. E. 2007, AJ, 661, 1129
- Wilson, R. E., 1979, AJ, 234, 1054
- Wilson, R. E., 1990, AJ, 356, 613
- Wilson, R. E., 2008, AJ, 672, 575
- Wilson, R. E., 2012, AJ, 144, 73

- Wilson, R.E., Devinney, E.J. 1971, AJ, 166, 605
- Wilson, R.E., Van Hamme, W., Terrell, D. 2010, AJ, 723, 1469
- Wolf, M., Diethelm, R. 1992, AcA, 42, 363
- Wunder, E., Wieck, M., Kilinc, B. et al. 1992, IBVS, 3760, 1W
- Yang, Y., Liu, Q. 2000, Ap&SS, 274, 799
- Yilmaz, M. et al. 2009, IBVS, 5887,1
- Zhu, L. Y.; Qian, S. B.; Soonthornthum, B.; He, J. J.; Liu, L., 2011, AJ, 142, 124Z
- Zhu, L. Y.; Zhao, E. G.; Zhou, X., 2016, RAA, 16, 68Z